

Phase separation and polymer interactions in aqueous poly(vinyl alcohol)/hydroxypropyl methylcellulose blends

P. Sakellariou*

ICI Paints, Research Department, Wexham Road, Slough, Berkshire, SL2 5DS, UK

and A. Hassan

University of Manchester, Institute of Science and Technology, Materials Science Centre, Manchester, M60 1QD, UK

and R. C. Rowe

ICI Pharmaceuticals, Alderley Park, Macclesfield, Cheshire, SK10 2TG, UK

(Received 21 February 1992; revised 13 July 1992)

This paper discusses the compatibility of aqueous hydroxypropyl methylcellulose (HPMC)/poly(vinyl alcohol) (PVA) blended systems. Dynamic mechanical analysis and differential scanning calorimetry have provided clear evidence of two phases. Each phase precluded almost completely the other component. The HPMC-rich phase was amorphous with a constant T_g , while the PVA-rich phase showed a limited level of crystallinity and a constant T_g for the amorphous part. Fourier-transform infra-red studies indicated hydrogen-bonding interactions involving the carbonyl and hydroxyl groups of like molecules but no detectable interactions between HPMC and PVA. A new hydrogen-bonding environment of the hydroxyls was observed in the blended system but was not capable of inducing any compatibility. The gross incompatibility was successfully predicted by the total solubility parameters of the two polymers and attributed to significant differences in the polar and hydrogen-bonding contributions. Surface energy analysis corroborated the inability of the two chains to participate in acid-base interactions between unlike molecules due to significant discrepancies in their Lewis acid-base characteristics. Finally, determination of the free energy of polymer-polymer interaction in water allowed approximate calculation of the Flory-Huggins parameters of aqueous PVA and HPMC systems.

(Keywords: aqueous; poly(vinyl alcohol); hydroxypropyl methylcellulose; blends; compatibility; interactions; morphology; solubility parameters; surface energy)

INTRODUCTION

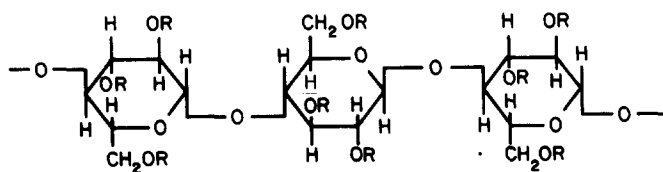
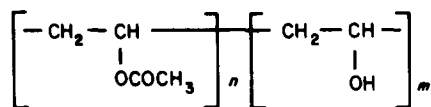
Aqueous polymeric systems are attracting increasing attention, not only for their strong relevance to biological systems but also for the current pressing need for solvent replacement for environmental reasons¹. Despite their wide application in a variety of materials, relatively little is known about the thermodynamic properties of these systems. This is particularly the case for aqueous polymer blends. The conventional and quite practicable Flory-Huggins approach cannot account for their behaviour², as phase behaviour is controlled by strong specific and highly directional interactions. Prausnitz³ has provided a brief but rather comprehensive review of recent efforts on the thermodynamics of aqueous polymer solutions. The same author has presented a new approach to the phase behaviour of these systems³.

In terms of solid-state phase behaviour of polar polymers, Coleman and coworkers⁴⁻⁶ have reported a new approach based on an association model. Separating

the free energy of mixing into non-hydrogen-bonding and hydrogen-bonding parts, they have successfully predicted the solid-state phase behaviour of a series of blends of poly(vinyl phenol) with carbonyl-group-containing homopolymers and copolymers. However, application of this approach is at present restricted to systems containing vinyl phenol owing to limited experimental information on hydroxyl group association. This is one of several attempts to account for polymer solubility and compatibility by splitting the overall contribution into a general dispersive term and an acid-base one^{7,8}. Partial solubility parameters and surface energy have been used to express these interactions⁹.

In this paper we report on an aqueous blend of two polar and hydrogen-bonding-group-containing polymers, hydroxypropyl methylcellulose (HPMC) and poly(vinyl alcohol) (PVA). They are used extensively in the film coating of solid dosage formulations (e.g. tablets). Carbonyl, ether oxygen and hydroxyl groups allow for inter- and intramolecular interactions between the two chains. We have studied the compatibility

* To whom correspondence should be addressed

Scheme 1 HPMC; R=H, CH₃, CH₂CH(OH)CH₃

Scheme 2 PVA

of the two polymers in the solid state by means of dynamic mechanical analysis, differential scanning calorimetry, infra-red spectroscopy and phase-contrast optical microscopy. We have also constructed the phase diagram of the ternary system HPMC/PVA/water, at room temperature. Finally, the nature and strength of polymer interactions have been investigated by means of surface energy measurements and related to polymer compatibility.

EXPERIMENTAL

Materials

Hydroxypropyl methylcellulose (HPMC; Pharmacoat 606) was supplied by Shin Etsu Chemical Co., Japan, with \bar{M}_n of 60.1 kg mol⁻¹ (Scheme 1).

Poly(vinyl alcohol) (PVA; Poval 205) was supplied by Kuraray Co., Japan (Scheme 2). It was 88% hydrolysed with a viscosity of 4.5–5.4 cP in 4% aqueous solutions at 20°C. Table 1 summarizes molecular weights and polydispersities for both polymers, determined by gel permeation chromatography with tetrahydrofuran (THF) as the carrier solvent and polystyrene (PS) standards calibration; quoted molecular weights are, therefore, approximate. Distilled water was used as the solvent. Polymer dissolution required slight heating (40°C).

Techniques

Torsional braid analysis. The dynamic mechanical spectra were obtained by torsional braid analysis (t.b.a.). This is a sensitive torsional pendulum, which monitors the response of a polymer-impregnated multifilament glass braid to a sinusoidal stress with temperature at a relatively constant frequency¹⁰. The dynamic mechanical spectra were recorded at ca. 1 Hz over the temperature range from -40 to 200°C and at a heating rate of 1°C min⁻¹. Glass braids consisted of two heat-cleaned glass yarns doubled to produce about 2½ turns per inch (~1 turn/cm) and secured between two butt-type clamps.

Heat-cleaned (500°C, 1 h) glass braids were immersed in polymer solutions (10% w/v) for 4 h, excess polymer was removed, and braids were dried at room temperature until touch-dry and under vacuum at 50°C until constant weight. Samples were stored over silica gel until tested.

Differential scanning calorimetry. About 5 mg of sample was accurately weighed in pierced, crimped aluminium pans and tested by means of Du Pont 912 dual-cell calorimeter at 10°C min⁻¹ under a nitrogen

atmosphere. Thermograms were recorded with the original samples (as cast) from room temperature to 270°C. Samples were then kept at 210°C for 10 min, quench-cooled with liquid nitrogen to room temperature and re-run to 270°C at 10°C min⁻¹. Duplicate measurements were made with very satisfactory reproducibility.

Fourier-transform infra-red analysis. FTi.r. analysis was performed by means of a Bruker spectrometer at a resolution of 2 cm⁻¹. Samples were thin films spread on KBr discs from 1% w/v aqueous solutions, dried under vacuum at 100°C overnight and stored in tightly sealed jars until tested. Infra-red spectra were recorded at 200°C and the final spectra were the average of 20 scans. The spectra were quantified by means of a curve-fitting program, which carried out least-squares fitting of a set of polynomial or Lorentzian curves to the spectra.

Surface energy analysis. Contact angles of distilled water, ethylene glycol and n-hexane on PVA and HPMC films were measured with the Willhelmy plate technique by means of the Dynamic Contact Angle Analyser, DCA-312. Microscope coverslips were coated with 10% w/v polymer solutions, dried at 100°C under vacuum overnight and stored over dried silica gel until used. The instrument monitors very accurately (± 0.1 mg) the force exerted on the sample while being immersed in a testing liquid (probe). Correction for the buoyancy force was implemented by means of the force at zero depth immersion. Samples were tested at a slow speed of 10 μ m min⁻¹ and at room temperature. Testing liquids were h.p.l.c. grade supplied by Aldrich. The advancing contact angles were used for the calculation of the surface energy.

Phase diagrams. The phase diagram of the ternary system PVA/HPMC/water was obtained by titrating heterogeneous systems with distilled water at room temperature, as described elsewhere^{11,12}.

Optical microscopy. Phase-contrast microscopy was used to study blend morphology. Thin sections (10–15 μ m) were microtomed with a glass knife from thick films (200 μ m) cast in Petri dishes. Thin films, cast directly from dilute solutions onto microscope slides, were also used.

RESULTS AND DISCUSSION

Dynamic mechanical analysis

Figure 1 illustrates the t.b.a. spectra for PVA/HPMC blends, as well as those of the two homopolymers. The T_g of HPMC, taken as $T(\log \text{decrement})_{\text{max}}$, was 159°C, in agreement with earlier work (158.5°C) on t.b.a. samples cast from equal volumes of methanol and methylene chloride¹³. The transition peak was sharp, characteristic of a one-phase system (Figure 1a).

A sharp transition was also recorded for PVA at 79°C

Table 1 Molecular weights (kg mol⁻¹) and polydispersity of HPMC and PVA

Polymer	\bar{M}_n	\bar{M}_w	\bar{M}_z	\bar{M}_w/\bar{M}_n
HPMC	60.1	133.4	287.3	2.2
PVA	73.9	127.8	213.8	1.7

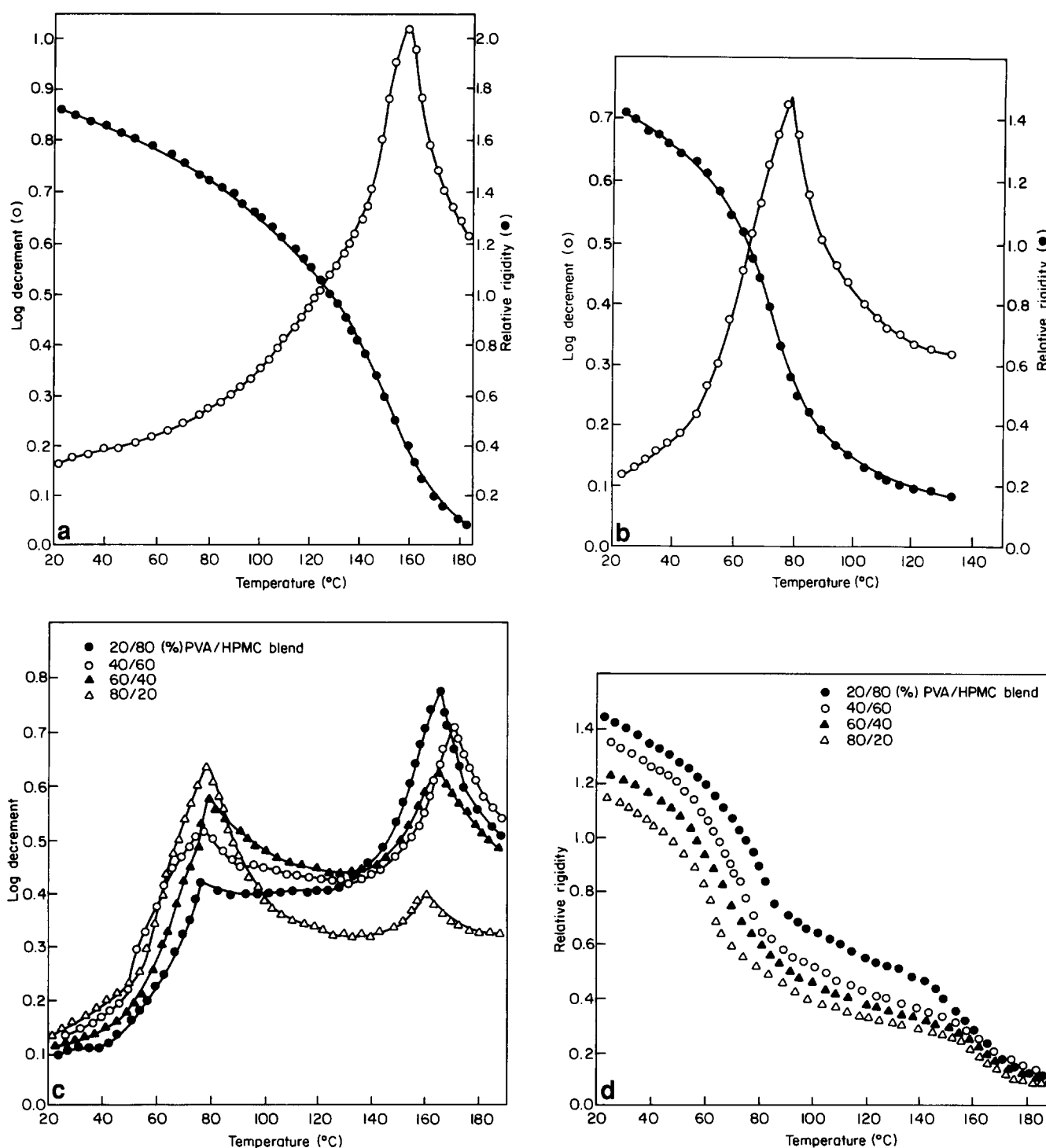


Figure 1 Dynamic mechanical spectra of (a) HPMC, (b) PVA and (c), (d) PVA/HPMC blends

(Figure 1b). A value of 88°C has been reported by Ciemniecki and Glasser¹⁴ for poly(vinyl acetate) 98% hydrolysed and determined by the dynamic mechanical analyser (d.m.t.a.) technique at 1 Hz and heating rate of 5°C min⁻¹. They also reported the presence of a single sharp transition. The two values are rather consistent in view of the significant difference in the degree of hydrolysis of the two chains (10%) and rates of heating employed. Both factors would tend to increase the T_g of our sample.

No relaxation was observed in the t.b.a. spectra at sub-ambient temperatures, -40 to 20°C. This suggests that there was no detectable crystallinity in PVA under

the conditions used for sample preparation in the t.b.a. experiments.

Two α -relaxations, close to the T_g of the corresponding homopolymers, were observed for the blends (Figures 1c and 1d). The height of each logarithmic decrement peak increased with the concentration of the corresponding component in the blend. A similar trend was observed in the relative rigidity curves. Figure 2 illustrates the variation of the T_g of each phase with blend composition. Within experimental error, both T_g values remained constant with varying blend composition. The same figure illustrates the expected behaviour of the corresponding one-phase system predicted by Fox¹⁵ and

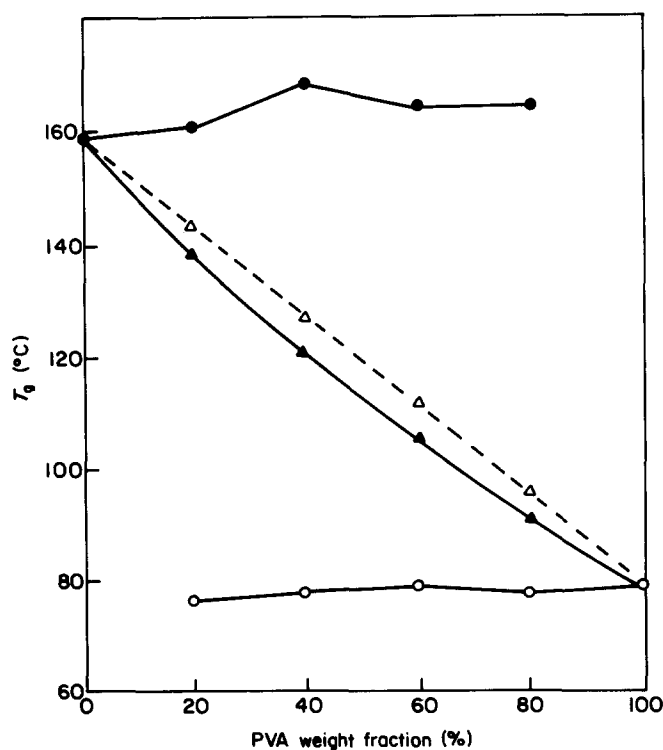


Figure 2 Variation of experimental (○, ●) and calculated (△, ▲) glass transition temperatures of PVA/HPMC blends with blend composition: (○) PVA-rich phase; (●) HPMC-rich phase; (△) Fox equation¹⁵; (▲) Gordon-Taylor equation¹⁶

Gordon-Taylor equations¹⁶. The transition breadth of the log decrement peaks increased significantly for the middle compositions, indicating a broader spectrum of relaxation times. Again, no evidence for crystallization or melting was observed in the t.b.a. spectra for the blended systems.

D.s.c. analysis

D.s.c. thermograms showed the presence of a broad endotherm at around 100°C attributed to evaporation of water (Figure 3a), obscuring the transition due to the PVA-rich phase at about 70°C. A sharper endotherm at 196°C was also recorded. The enthalpy associated with this endotherm (ΔH , Table 2) increased with increasing PVA content in the blend, while its position remained unaltered. This is consistent with melting of PVA crystalline phases. The insensitivity of melting temperature (T_m) to blend composition indicates the absence of any interactions between HPMC and PVA. This is in agreement with the t.b.a. data. The transition due to the HPMC-rich phase was obscured by the melting endotherm.

On annealing the sample at temperatures (210°C) above the T_g of both phases, the melting endotherm at 196°C disappeared (Figure 3b), suggesting that the amorphous matrix did not crystallize under the conditions employed (10°C min⁻¹). This is in contrast with earlier reports¹⁷ of crystallinity following 10 min annealing at 125°C. At the same time, the broad endotherm, due to water evaporation, disappeared as expected. This enabled determination of the glass transition due to the PVA-rich phase, which was located at 71°C and remained constant through blend composition. The T_g of this phase was some 8°C lower

than that determined by the t.b.a., in agreement with the expected behaviour¹³. The transition due to the HPMC-rich phase, in the range 150–175°C, could not be accurately resolved from the thermogram baseline. The d.s.c. data suggest gross incompatibility between the two polymers in the solid state.

Infra-red analysis

Our discussion will concentrate on the hydroxyl and carbonyl stretching vibration bands, as they are expected to be affected by hydrogen-bonding interactions and are most amenable to quantitative analysis. I.r. spectra were obtained at a temperature above the T_g of both blend

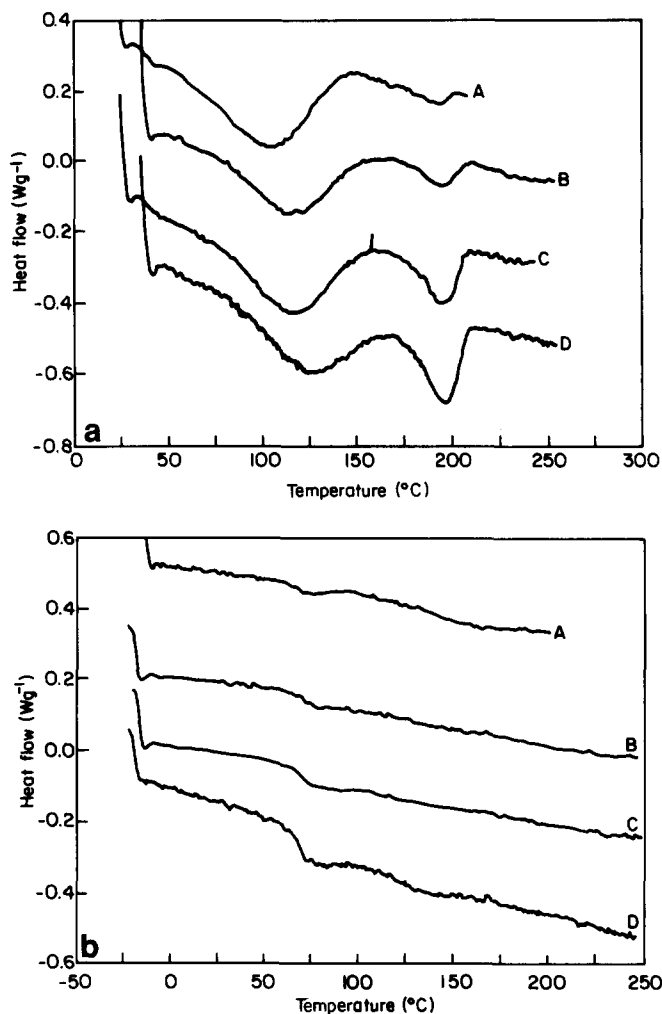


Figure 3 (a) D.s.c. thermograms of PVA/HPMC blends as cast. (b) D.s.c. thermograms annealed at 210°C for 10 min and quench-cooled. Curves: (A) 22/78, (B) 47/53, (C) 52/48 and (D) 77/23 PVA/HPMC

Table 2 D.s.c. data of HPMC/PVA blends

PVA (%)	ΔH^a (J g ⁻¹)	T_m (°C)	T_g^b (°C)	ΔH^c (J g ⁻¹)
22	5	195	71	6.31
47	8.2	195	71	7.26
52	17.4	195	71	9.45
77	24.1	197	71	—
100	24.2	197	—	33.60

^a As cast, 10°C min⁻¹ (run 1)

^b After annealing (run 2)

^c York and Okhamafe¹⁷

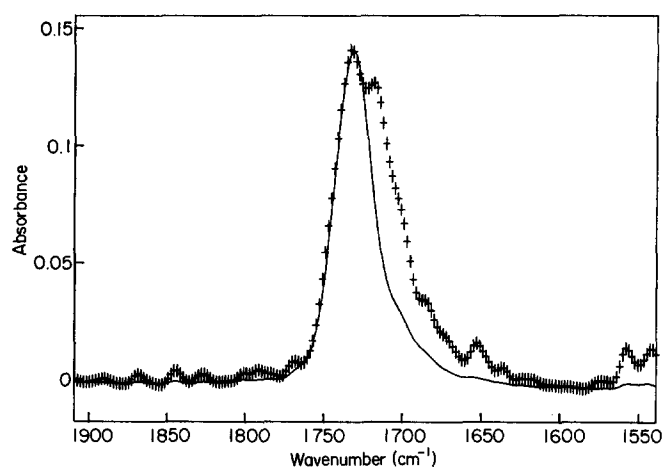


Figure 4 Infra-red spectra of PVA (+) and 50/50 PVA/HPMC blend (-) in the carbonyl stretching region

constituents (200°C) to ascertain equilibrium and remove contributions from free and bonded water.

Figure 4 shows the i.r. spectra of PVA and the 50/50 w/w PVA/HPMC blend, focused on the ester carbonyl stretching vibration region at 200°C. Two bands were observed at 1736 and 1719 cm^{-1} for PVA. In accordance with results by Coleman *et al.*^{18,19} and Cesteros *et al.*²⁰, these two bands were assigned to 'free' unassociated and to associated hydrogen-bonded carbonyl groups in the sample, respectively. The relative proportion of free and associated carbonyl groups was calculated from the area under the vibration peaks (A) normalized for the absorptivity of the two groups (α)²¹:

$$F_H = \frac{A_H}{A_H + A_F/\alpha_r} \quad (1)$$

where subscripts H and F denote the hydrogen-bonded and 'free' unassociated carbonyl groups, respectively, and α_r is defined as the ratio of the absorbance coefficients of bonded to 'free' groups, $\alpha_r = \alpha_H/\alpha_F$. Coleman *et al.*¹⁸ reported a value of 1.5 for α_r . The relative fraction of hydrogen-bonded carbonyl groups was calculated to be 0.71. The frequency shift from hydrogen-bonded to 'free' carbonyl groups, 19 cm^{-1} , was lower than that reported²⁰ for poly(*N*-vinylpyrrolidone)/poly(monobenzyl itaconate) blends (45 cm^{-1}) and comparable to that for poly(vinyl phenol)^{18,22} with a series of poly(alkyl methacrylate) blends (ca. 27 cm^{-1}).

The shape of the carbonyl band for the PVA/HPMC blend (Figure 4) was different from that of the PVA homopolymer, indicating a change in the balance of free and associated carbonyl groups in the blend. The spectrum of the blend in the carbonyl stretching region showed two bands at 1732 and 1706 cm^{-1} assigned to 'free' and associated carbonyls, respectively. The relative fraction of hydrogen-bonded carbonyls, calculated with equation (1), was lower than that of PVA alone, $F_H = 0.15$, indicating the presence of a relatively increased number of free carbonyls in the blend.

Figure 5 illustrates the hydroxyl vibration region of the PVA, HPMC and PVA/HPMC blend spectra. The C-H stretching vibration bands are also included in this figure to account for film thickness variation. A broad band was observed at around 3431 cm^{-1} for PVA, indicating the presence of a broad range of associated hydroxyls. The band was fitted successfully to a single

polynomial function, corroborating the presence of a broad but single associated hydroxyls population. The persistence of hydrogen-bonded carbonyl groups at temperatures well in excess of 100°C indicates the presence of intermolecular interactions between carbonyl groups and hydroxyls of different PVA chains.

The shape of the OH vibration stretching region of the HPMC band (Figure 5) was sharper than that of PVA and was satisfactorily fitted to two polynomials corresponding to free (3475 cm^{-1}) and bonded (3315 cm^{-1}) hydroxyls. The hydroxyl vibration stretching for the blend (Figure 5) was characterized by a broad band, which was successfully fitted to two polynomial curves. The two bands were assigned to free (3469 cm^{-1}) and associated hydroxyls (3327 cm^{-1}), with the bonded hydroxyls prevailing. The fact that the hydroxyl band can be deconvoluted to two bands at frequencies representative of a free and a bonded environment has been taken as an indication for the presence of two hydroxyl populations in the system²¹, with the free hydroxyls in excess of the bonded ones. The deconvoluted band due to the associated hydroxyls shifted to lower frequencies compared to PVA, indicating changes in H-bond environment and perhaps the presence of new interactions. These interactions would involve almost exclusively the hydroxyls with no participation of the PVA carbonyl groups, as shown by the reduced fraction of bonded carbonyls in the blend.

Table 3 Surface energy and solubility parameters of HPMC and PVA. Symbols are explained in the text

Polymer	HPMC	PVA
δ_{1w}^+	0.2791	0.1979
δ_{1w}^-	0.4127	0.7164
ΔG_{212} (mJ m^{-2})	-43.2	-23.2
γ^+ (mJ m^{-2})	1.9	1.0
γ^- (mJ m^{-2})	4.4	13.1
γ^d (mJ m^{-2})	18.4	18.4
δ ($\text{MPa}^{1/2}$)	22.8	32.7
δ_d ($\text{MPa}^{1/2}$)	14.4	16.4
δ_p ($\text{MPa}^{1/2}$)	5.8	14.7
δ_h ($\text{MPa}^{1/2}$)	16.7	24.2
x_p	0.77	0.87

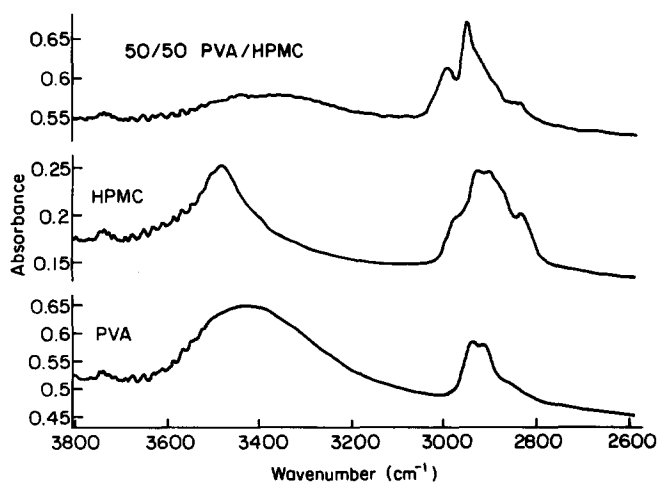


Figure 5 Infra-red spectra for PVA, HPMC and 50/50 PVA/HPMC blend in the hydroxyl vibration region

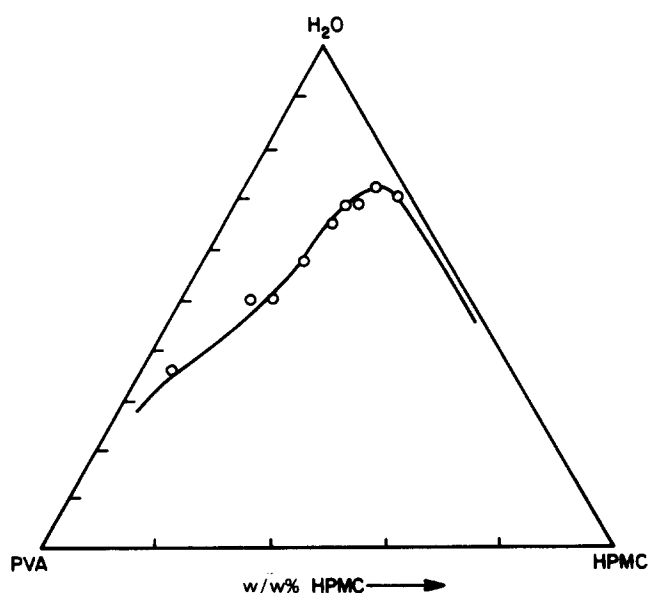


Figure 6 Phase diagram of PVA/HPMC/H₂O ternary system at room temperature

In view of the d.s.c. and t.b.a. data, these interactions are not sufficient to introduce compatibility in the system.

Phase diagram

Figure 6 illustrates the phase diagram of the PVA/HPMC/H₂O system at room temperature. The binodal was not symmetrical, indicating a preferential solubility of PVA in water, compared to HPMC at this temperature. Polymer solutions at higher concentrations were extremely viscous and could not be tested reliably. The plait point was located at 5.6% w/v polymer concentration for blends with ca. 80% HPMC. The Flory–Huggins interaction parameter at the plait point can be calculated from equation (2) derived by Tompa²³:

$$\chi_{23}^{\text{pl}} = \frac{1}{2}(x_2^{-1/2} + x_3^{-1/2})^2(1 - \phi_1)^{-1} \quad (2)$$

where x is the number of polymer segments and ϕ is the volume fraction; subscripts 1, 2 and 3 correspond to water, PVA and HPMC respectively. A value of 0.005 was calculated from equation (2).

The enthalpic part of the polymer–polymer interaction parameter can be calculated from the Hildebrand–Scatchard theory²⁴:

$$\chi_{23} = V_r(\delta_2 - \delta_3)^2/RT \quad (3)$$

where δ is the solubility parameter and V_r is the reference molar volume. Table 3 lists the total and partial solubility parameters as well as the polarity and surface energy for the two polymers. Comparison of the blend interaction parameter with its critical parameter has been quite successful in predicting compatibility^{11,25}:

$$\chi_{\text{crit}} = \frac{1}{2}(x_2^{-1/2} + x_3^{-1/2})^2 \quad (4)$$

A value of 3.3×10^{-4} was calculated from equation (4).

The sizeable difference between the calculated values for χ_{23} from equation (3) (3.906) and χ_{crit} indicates significant incompatibility in the system, in agreement with the dynamic mechanical and infra-red data. The partial solubility parameters (Table 3) can elucidate the underlying reasons for this incompatibility. The dispersive component δ_d is similar for both polymers, as expected. Incompatibility seems to arise from strong

mismatch between the hydrogen-bonding terms, δ_h , as well as the general polar component, δ_p . The solubility parameter approach is unable to deconvolute the acidic contribution to the hydrogen-bonding interaction from the basic contribution. A first attempt to elucidate this aspect will be presented later in the paper in terms of surface energy. We are developing a new approach to this problem based on solvation constants²⁶, which will be reported for this system in a future publication. Finally, PVA was significantly more polar than HPMC.

Blend morphology

Figures 7 and 8 show the phase-contrast optical micrographs for microtomed sections and thin films of the PVA/HPMC blends respectively. The morphology was characteristic of a grossly phase-separated system, with a broad distribution of minor-phase dispersion within the major-component matrix. Morphologies throughout the blend composition range were typical of a nucleation and growth mechanism. The average size of the dispersed phase was ca. 10 μm . Microtomed specimens, reflecting more accurately the bulk film behaviour, showed a broad distribution of dispersed phase size extending from 5 to 20 μm . The average size of the dispersed phase appeared larger for blends with significant PVA weight fractions. Although the samples were not annealed at temperatures above the T_g of both homopolymers, the FTi.r. data did not produce evidence for significant changes in the interactions at high temperatures (200°C).

Surface energy analysis

Following the development of a methodology for determining the electron-donor (Lewis base, γ^-) and electron-acceptor (Lewis acid, γ^+) components of the surface energy, Van Oss and coworkers^{27–29} used the Girifalco equation³⁰ to express the free energy of polymer–solvent and polymer–polymer interactions in the presence of solvent for polar systems.

The free energy of interaction of a bipolar polymer (2) in water (1) is given by:

$$\begin{aligned} \Delta G_{212} = & -2[(\gamma_1^d)^{1/2} - (\gamma_2^d)^{1/2}]^2 \\ & -4[(\gamma_1^+ \gamma_1^-)^{1/2} + (\gamma_2^+ \gamma_2^-)^{1/2} - (\gamma_1^+ \gamma_2^-)^{1/2} - (\gamma_1^- \gamma_2^+)^{1/2}] \end{aligned} \quad (5)$$

The first part of the expression includes the dispersive component (van der Waals forces) while the second part accounts for the Lewis acid–base interactions. The polymers are assumed at this stage to be bipolar in that they exhibit both electron-donor and electron-acceptor properties. Using Flory's definition of the polymer–solvent interaction parameter², we can convert the free energy of interaction into the familiar Flory–Huggins interaction parameter:

$$\chi_{12} = -S_c \Delta G_{212}/kT \quad (6)$$

where S_c is the minimum contactable surface area for polymer–polymer interactions. It must be noted that the definition of χ_{12} in equation (6) involved the free energy rather than the enthalpy of mixing used in the original Flory definition². This is consistent with later extension of χ_{12} to a free-energy term by Flory to account for accumulating experimental evidence. The values of χ_{12} calculated from equation (6) will, therefore, include an

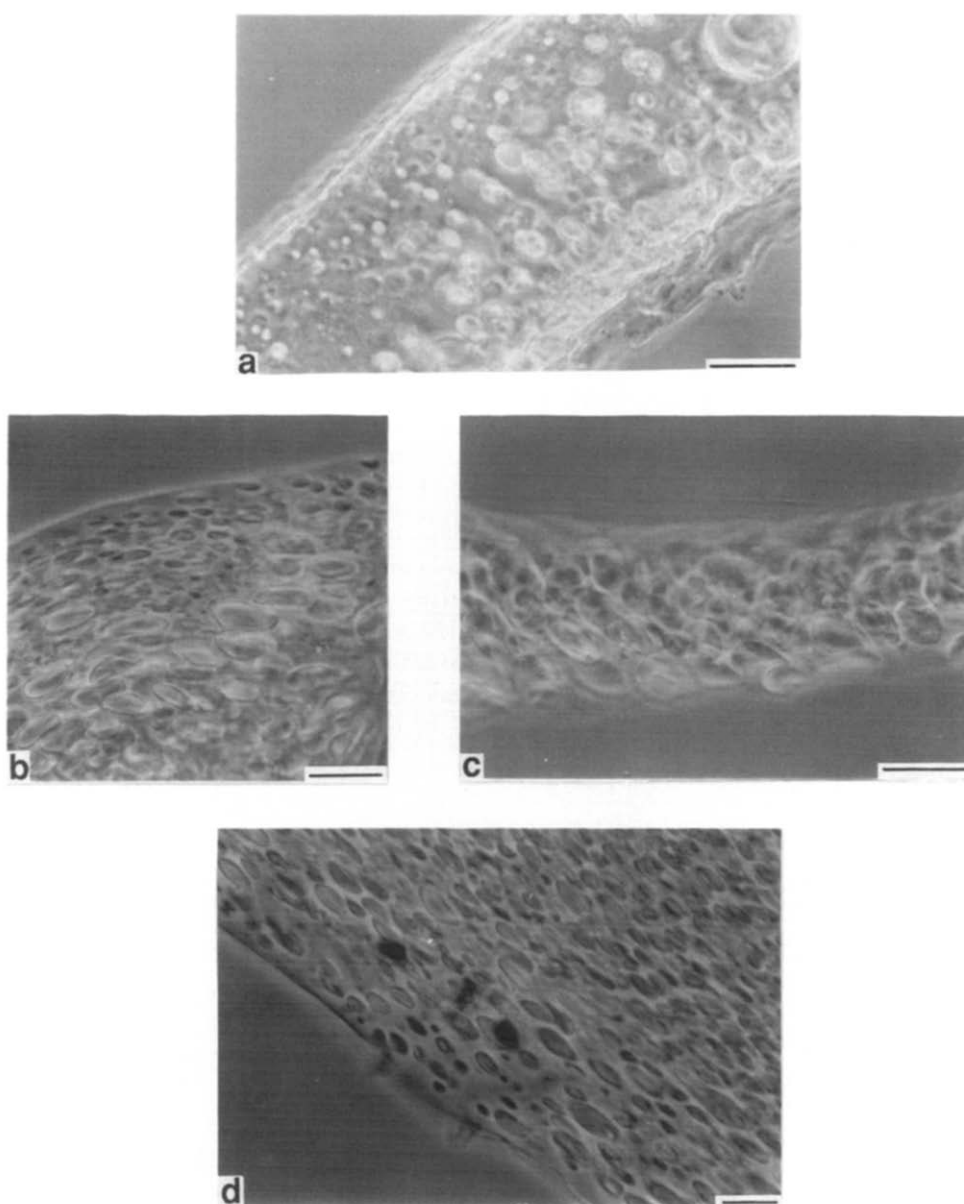


Figure 7 Optical micrographs of microtomed sections of PVA/HPMC blends cut normal to the bulk film surface: (a) 77/23, (b) 52/48, (c) 41/59 and (d) 22/78 PVA/HPMC. In each case the scale bar represents 10 μm

entropic contribution. This is particularly important in the case of aqueous systems where changes in the entropy of mixing can have a significant effect on the phase behaviour.

The procedure followed involved measuring the contact angle of three liquids (probes) on films of the two homopolymers. The probes were n-hexane, glycerol and water. The hydrocarbon contact angle (θ_H) affords calculation of the general van der Waals component:

$$\gamma_2^d = \gamma_1(1 + \cos \theta_H)^2/4 \quad (7)$$

Table 4 lists all relevant parameters of the three probes.

Calculation of the free energy of polymer interaction requires knowledge of the Lewis acid–base contributions to the surface energy. This was implemented by means of the relative fractional polarity²⁷:

$$\begin{aligned} \delta_{iW}^+ &= \gamma_i^+ / \gamma_W^+ \\ \delta_{iW}^- &= \gamma_i^- / \gamma_W^- \end{aligned} \quad (8)$$

Subscripts W and G denote water and glycerol,

respectively. It has been determined²⁷ that:

$$\gamma_W^+ \gamma_W^- = 51 \text{ mJ m}^{-2} \quad (9)$$

$$\gamma_G^+ \gamma_G^- = 30 \text{ mJ m}^{-2} \quad (10)$$

From the interfacial tension between water and glycerol, the relative fractional polarity was determined by the same group:

$$\delta_{GW}^+ = 0.471 \quad \text{and} \quad \delta_{GW}^- = 1.245$$

Rearrangement of the original Girifalco expression gives two equations for the two remaining probes with two unknowns, δ_{1W}^+ and δ_{1W}^- :

$$(1 + \cos \theta_W) \gamma_W = 2(\gamma_1^d \gamma_W^d)^{1/2} + 51 \delta_{1W}^+ + 51 \delta_{1W}^- \quad (11)$$

$$(1 + \cos \theta_G) \gamma_G = 2(\gamma_1^d \gamma_G^d)^{1/2} + 63.5 \delta_{1W}^+ + 24 \delta_{1W}^- \quad (12)$$

Table 3 summarizes the basic parameters of PVA and HPMC calculated with this procedure.

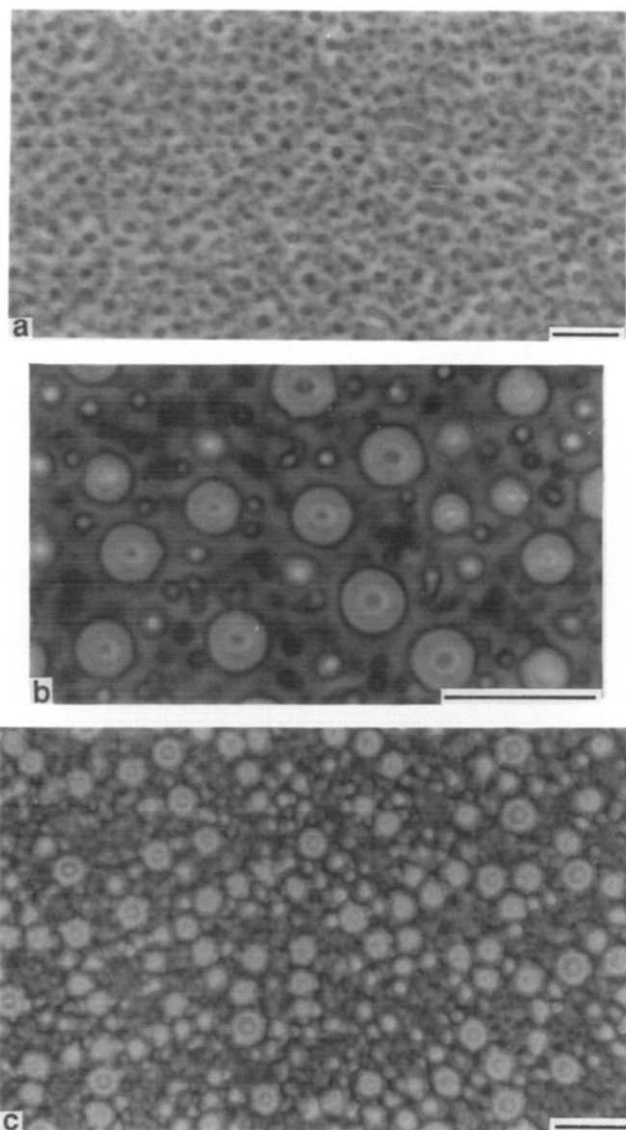


Figure 8 Optical micrographs of thin films cast from dilute solutions on microscope slides at room temperature: (a) 22/78, (b) 77/23 and (c) 61/59 PVA/HPMC

The general dispersive term, γ^d , for HPMC was in good agreement with the value determined by Rowe³¹ and significantly lower than that of cellulose acetate³², 38 mJ m^{-2} . The free energy of interaction between polymer segments in water, ΔG_{212} , was significantly lower for HPMC (-43.2 mJ m^{-2}) than PVA (-23.3 mJ m^{-2}). This would suggest a stronger propensity of HPMC segments to interact with each other in an aqueous environment. Conversion to conventional χ_{12} requires consideration of the average cross-sectional area for this interaction. PVA showed nearly monopolar behaviour (Table 3) with significantly stronger Lewis-base characteristics (γ^-) in agreement with literature data for the fully hydrolysed polymer²⁸. HPMC was also characterized by a stronger Lewis-base component but its behaviour was relatively more dipolar than that of PVA (Table 3). This is consistent with relative fractional polarities determined by the three-dimensional solubility parameters. The acid–base characterization of the two chains corroborates the relative inability of the two chains to participate in intermolecular hydrogen bonding. This is primarily the result of the predominantly basic

nature of both chains coupled with very weak acid characteristics.

The cross-correlation of the Lewis-acid and Lewis-base characteristics of polymer chains in aqueous systems adds to recent observations by Cowie and coworkers^{33,34}. Adopting Tanford's³⁵ approach to the hydrophobic effect, they assigned the observed lower critical solution temperature (LCST) to changes in the polar and hydrophobic interaction balance in mixtures of poly(acrylic acid)/dioxane/water. To distinguish from the conventional LCST, arising from free-energy differences, they described the experimental boundary as a quasi-LCST. Adequate accounts of the behaviour of aqueous multicomponent systems require more accurate specification of the polar interactions in terms of their acid–base characteristics.

Determination of the free energy of interaction between polymer segments in water, ΔG_{212} , allows calculation of the polymer–solvent interaction parameter χ_{12} according to equation (6). This requires knowledge of the minimum contactable surface between polymer segments, S_c . The diameter of the reptation tube for the two chains was calculated approximately by means of simple molecular modelling packages. Approximate values of 3 and 12 Å were computed for the reptation tube diameters for PVA and HPMC, respectively. Incorporation of these two values into equation (6) gave values of 0.40 and 11.9 for χ_{12} for PVA and HPMC, respectively. Although the computed reptation tube diameter for PVA produced a satisfactory approximation to S_c , that of HPMC produced an unacceptably high χ_{12} value. It would not be unreasonable to assume that the substituents on the anhydroglucose unit of HPMC are mainly responsible for polymer–polymer interactions in water. Our calculation, therefore, which took into consideration the whole unit, would be a gross overestimate. For instance, if the value for PVA was assigned to the minimum contactable area for HPMC, χ_{12} is calculated to be 0.7. This value is more consistent with literature data. Both polymers exhibit LCST behaviour. HPMC has an LCST of 52°C ³⁶ while that of PVA, although not accurately determined, lies well above this temperature¹⁴. This was also reflected in the shape of the experimentally determined coexistence curve.

CONCLUSIONS

Blends of HPMC with PVA have been shown to be incompatible when cast from aqueous solutions despite the presence of groups capable of hydrogen bonding. Incompatibility persisted even after annealing at temperatures well above the glass transition temperatures of both polymers (200°C). The PVA-rich phases developed limited crystallinity during film casting, which largely disappeared when annealed at high temperatures and quenched-cooled.

FTi.r. studies elucidated the hydrogen-bonding

Table 4 Surface energy (mJ m^{-2}) of probes used to characterize the polymers

Probe	γ^d	γ^p	γ
Water	21.8 ± 0.7	51.0	72.8
Glycerol	37.0 ± 4.0	23.4	53.4
n-Hexane	18.4	0.0	18.4

interactions involving the carbonyl and hydroxyl groups of the two polymers in the blended system. Evidence for reduced association of the PVA carbonyls in the blended system was obtained. Only ca. 15% of the carbonyl groups, compared to ca. 70% in the case of PVA homopolymer, remained hydrogen bonded even at temperatures as high as 200°C. These interactions were attributed to hydrogen bonding involving the carbonyl and hydroxyl groups between like chains, giving rise to gross incompatibility all over the temperature range from 30 to 200°C. In terms of the hydroxyls of PVA and HPMC, the blend contained free and associated groups. This was consistent with the HPMC behaviour but contrary to that of the PVA, which showed a broad population of bonded hydroxyls with no detectable free hydroxyls. No significant changes in the frequency of the deconvoluted band due to the associated hydroxyls was observed with increasing temperature, indicating that the incompatibility was not solvent-induced and a product of non-equilibrium conditions. The balance of free to associated hydroxyls remained unchanged with increasing temperature and comparable to that of the HPMC homopolymer. A new hydrogen-bonding environment and some new interactions involving the hydroxyls were observed in the blended system in terms of a shift of the bonded hydroxyl band to lower frequencies.

The incompatibility of the two polymers was successfully predicted by the total solubility parameters using the Hildebrand–Scatchard theory. Furthermore, the reasons for the absence of significant intermolecular interactions between unlike molecules in the system were elucidated by the partial solubility parameters of the two polymers. Significant differences between the polar (δ_p), and in particular the hydrogen-bonding terms (δ_h), have been argued to be responsible. This argument was further substantiated by calculating the surface free energy of polymer–polymer interaction in water and the Lewis acid–base characteristics of the two homopolymers. The significant differences in the Lewis acid–base characteristics of the two polymers have been argued to preclude any acid–base interactions between PVA and HPMC, hence leading to gross incompatibility in the system. Incompatibility in the liquid state was found to be further exacerbated by significant differences in the solvent quality of water for the two polymers. This was reflected in the polymer–solvent interaction parameters for the two polymers, calculated from the free energy of polymer–solvent interactions.

REFERENCES

- 1 Eisenberg, H. *Eur. J. Biochem.* 1990, **187**, 7
- 2 Flory, P. in 'Principles in Polymer Chemistry', Cornell University Press, Ithaca, NY, 1951
- 3 Prange, M. M., Hooper, H. H. and Prausnitz, J. M. *AIChE J.* 1989, **35** (5), 803
- 4 Coleman, M. M., Lichkus, A. M. and Painter, P. C. *Macromolecules* 1989, **22**, 586
- 5 Painter, P. C., Park, Y. and Coleman, M. M. *Macromolecules* 1989, **22**, 570
- 5 Painter, P. C., Park, Y. and Coleman, M. M. *Macromolecules* 1989, **22**, 580
- 7 Van Oss, C. J., Chaudhury, M. J. K. and Good, R. J. *Chem. Rev.* 1988, **88**, 927
- 8 Fowkes, F. M. *Ind. Eng. Chem, Prod. Res. Dev.* 1978, **17**, 3
- 9 Barton, A. F. M. in 'Handbook of Solubility Parameters and Other Cohesion Parameters', CRC Press, Boca Raton, FL, 1983
- 10 Sakellariou, P., White, E. F. T. and Rowe, R. C. *Br. Polym. J.* 1987, **19**, 73
- 11 Sakellariou, P. and Rowe, R. C. *J. Appl. Polym. Sci.* 1991, **43**, 845
- 12 Sakellariou, P., Eastmond, G. C. and Miles, I. S. *Polymer* 1991, **32**, 2351
- 13 Sakellariou, P., Rowe, R. C. and White, E. F. T. *Int. J. Pharm.* 1986, **34**, 93
- 14 Ciemniecki, S. L. and Glasser, W. G. *Polymer* 1988, **29**, 1030; also Molyneaux, P. in 'Water-Soluble Polymers: Properties and Behaviour', CRC Press, Boca Raton, FL, 1983, Vol. I, Ch. 4
- 15 Fox, T. G. *Bull. Am. Phys. Soc.* 1923, **1**, 123 (J5)
- 16 Gordon, M. and Taylor, J. S. *J. Am. Chem. Soc.* 1952, **2**, 493
- 17 York, P. and Okhamafe, A. O. *Anal. Proc.* 1985, **22**, 40
- 18 Moskala, E. J., Varnell, D. F. and Coleman, M. M. *Polymer* 1985, **26**, 229
- 19 Coleman, M. M., Xu, Y., Painter, P. C. and Harrell, J. R. ESOPS Conf., Koln, September 1990; IUPAC Conf., Singapore, November 1990
- 20 Cesteros, L. C., Rego, J. M., Vazquez, J. J. and Katime, I. *Polym. Commun.* 1990, **31**, 152
- 21 Lee, Y. S., Painter, P. C. and Coleman, M. M. *Macromolecules* 1988, **21**, 346, 954; also Teragagni, P., Masetti, G. and Zerbi, G. *Chem. Phys.* 1978, **28**, 55
- 22 Serman, C. J., Painter, P. C. and Coleman, M. M. *Polymer* 1991, **32**, 1049
- 23 Tompa, H. in 'Polymer Solutions', Butterworths, London, 1956, Ch. 7
- 24 Hildebrand, J. H., Prausnitz, J. M. and Scott, R. R. in 'Regular and Related Solutions', Van Nostrand Reinhold, New York, 1970
- 25 Krause, S. in 'Polymer Blends' (Ed. D. R. Paul) Academic Press, New York, 1978, Vol. 1
- 26 Abraham, M. H., Whiting, G. S., Doherty, R. M., Shuely, W. J. and Sakellariou, P. *Polymer* 1992, **33**, 2162
- 27 Van Oss, C. J., Arnold, K., Good, R. J., Gawrisch, K. and Ohki, S. *J. Macromol. Sci., Chem. (A)* 1990, **27** (5), 563
- 28 Van Oss, C. J., Chaudhury, M. K. and Good, R. J. *Adv. Colloid Interface Sci.* 1987, **28**, 35
- 29 Van Oss, C. J., Chaudhury, M. K. and Good, R. J. *Separ. Sci. Technol.* 1989, **24** (1&2), 15
- 30 Good, R. J. and Girifalco, L. A. *J. Phys. Chem.* 1960, **64**, 561; *ibid.* 1957, **61**, 904
- 31 Rowe, R. C. *Int. J. Pharm.* 1989, **53**, 75
- 32 Van Oss, C. J., Good, R. J. and Chaudhury, M. K. *J. Chromatogr.* 1987, **53**, 391
- 33 Cowie, J. M. G. and Swinyard, B. *Br. Polym. J.* 1991, **25**, 109
- 34 Cowie, J. M. G. and Swinyard, B. *Polymer* 1990, **31**, 1507
- 35 Tanford, C. in 'The Hydrophobic Effect', Wiley, New York, 1973
- 36 Sakellariou, P. and Rowe, R. C. unpublished data